



**HAL**  
open science

## Linking Allele-Specific Expression And Natural Selection In Wild Populations

Romuald Laso-Jadart, Kevin Sugier, Emmanuelle Petit, Karine Labadie, Pierre Peterlongo, Christophe Ambroise, Patrick Wincker, Jean-Louis Jamet, Mohammed-Amin Madoui

► **To cite this version:**

Romuald Laso-Jadart, Kevin Sugier, Emmanuelle Petit, Karine Labadie, Pierre Peterlongo, et al.. Linking Allele-Specific Expression And Natural Selection In Wild Populations. 2019. hal-02275928

**HAL Id: hal-02275928**

**<https://inria.hal.science/hal-02275928>**

Preprint submitted on 2 Sep 2019

**HAL** is a multi-disciplinary open access archive for the deposit and dissemination of scientific research documents, whether they are published or not. The documents may come from teaching and research institutions in France or abroad, or from public or private research centers.

L'archive ouverte pluridisciplinaire **HAL**, est destinée au dépôt et à la diffusion de documents scientifiques de niveau recherche, publiés ou non, émanant des établissements d'enseignement et de recherche français ou étrangers, des laboratoires publics ou privés.

# 1 Linking Allele-Specific Expression And Natural 2 Selection In Wild Populations

3  
4 Romuald Laso-Jadart<sup>1,6\*</sup>, Kevin Sugier<sup>1</sup>, Emmanuelle Petit<sup>2</sup>, Karine Labadie<sup>2</sup>, Pierre Peterlongo<sup>3</sup>,  
5 Christophe Ambroise<sup>4</sup>, Patrick Wincker<sup>1,6</sup>, Jean-Louis Jamet<sup>5</sup>, Mohammed-Amin Madoui<sup>1,6\*</sup>

6  
7 <sup>1</sup>Génomique Métabolique, Genoscope, Institut François Jacob, CEA, CNRS, Univ Evry,  
8 Université Paris-Saclay, Evry, France.

9 <sup>2</sup>CEA, Genoscope, Institut de Biologie François Jacob, Université Paris-Saclay, Evry, 91057,  
10 France.

11 <sup>3</sup>Univ Rennes, CNRS, Inria, IRISA - UMR 6074, F-35000 Rennes.

12 <sup>4</sup>LaMME, CNRS, Univ Evry, Université Paris-Saclay, Evry, France

13 <sup>5</sup>Université de Toulon, Aix-Marseille Université, CNRS/INSU/IRD, Mediterranean Institute of  
14 Oceanology MIO UMR 110, CS 60584, 83041 Toulon cedex 9, France.

15 <sup>6</sup>Research Federation for the study of Global Ocean Systems Ecology and Evolution,  
16 FR2022/Tara Oceans GO-SEE, 3 rue Michel-Ange, 75016 Paris, France

17 \* Corresponding authors. Emails: [rlasojad@genoscope.cns.fr](mailto:rlasojad@genoscope.cns.fr) & [amadoui@genoscope.cns.fr](mailto:amadoui@genoscope.cns.fr)

## 18 **Abstract**

19 Allele-specific expression (ASE) is now a widely studied mechanism at cell, tissue and organism  
20 levels. However, population-level ASE and its evolutive impacts have still never been  
21 investigated. Here, we hypothesized a potential link between ASE and natural selection on the  
22 cosmopolitan copepod *Oithona similis*. We combined metagenomic and metatranscriptomic data  
23 from seven wild populations of the marine copepod *O. similis* sampled during the *Tara* Oceans  
24 expedition. We detected 587 single nucleotide variants (SNVs) under ASE and found a  
25 significant amount of 152 SNVs under ASE in at least one population and under selection across  
26 all the populations. This constitutes a first evidence that selection and ASE target more common  
27 loci than expected by chance, raising new questions about the nature of the evolutive links  
28 between the two mechanisms.

29

30

31

32

33

34

35

## 36 **Introduction**

37 Allele-specific expression (ASE), or allelic imbalance, refers to difference of expression between  
38 two alleles of a locus in a heterozygous genotype due to genetic or epigenetic polymorphism.  
39 Through DNA methylation or histone modifications, epigenetics could repress a disadvantageous  
40 or a specific parental allele, leading in some cases to monoallelic expression, as demonstrated in a  
41 variety of organisms including mouse, maize or bumblebee<sup>1-4</sup>. On the other hand, ASE may have  
42 a genetic origin through, for example, mutations in transcription factor binding sites<sup>5,6</sup>, or post-  
43 transcriptional mechanisms like non-sense mediated decay<sup>7-9</sup>. Recently, several studies led to a  
44 better understanding of ASE thanks to the development of advanced tools allowing their  
45 detection at the individual, tissue and cell levels<sup>7,9-15</sup>. ASE has been investigated in the context of  
46 *cis*- and *trans*-regulation of gene expression<sup>16</sup>, expression evolution<sup>17</sup> and association between  
47 gene expression and human diseases<sup>18</sup>. First approaches in natural populations of primates and  
48 flycatchers have been undertaken with individual-level data<sup>19-21</sup>. Moreover, studies began to  
49 question the relative contribution of genetics and environment on gene expression using ASE in  
50 human<sup>22-25</sup> and fruit flies<sup>26</sup>.

51 However, population-level ASE in several wild populations of one species and its potential  
52 evolutive origins and consequences remain largely uninvestigated. The need for numerous  
53 individual RNA-seq and whole-genome genotyping data constitutes the main obstacle for  
54 population-scale analyses. Today, the advances of next-generation sequencing technologies allow  
55 integrating large metagenomic and metatranscriptomic data from environmental samples, and  
56 new approaches can now be considered using whole population information.

57 In natural populations, we expect most loci to be under neutral evolution and balanced expression  
58 (Fig. 1a)<sup>27,28</sup>. When selection occurs on a specific locus, the selected allele tends to homozygosity

59 creating a specific population-level expression pattern of the selected allele (Fig.1b).In the  
60 absence of selection, if the same allele is favored by ASE in most of the individuals, the observed  
61 population-level expression pattern (Fig. 1c) will be similar to the one observed in the case of  
62 selection (Fig.1b).Considering that both mechanisms impact fitness, we hypothesized that ASE  
63 and natural selection could preferentially target the same loci, in different populations, showing a  
64 possible link between the two mechanisms.

65 In this study, we focus on the widespread epipelagic, temperate and cold water small-sized  
66 copepod, *Oithona similis* (Cyclopoida, Claus 1866), notably known to be highly abundant in  
67 Arctic<sup>30-33</sup>. Copepods, and particularly *Oithona*, are small crustaceans forming the most abundant  
68 metazoan on Earth, reflecting strong adaptive capacities to environmental fluctuations<sup>34-36</sup>.They  
69 play a key ecological role in biogeochemical cycles and in the marine trophic food chain<sup>37</sup>;  
70 therefore copepods constitute an ideal model to study wild population evolution<sup>38-41</sup>

71 The first goal of our study was to identify loci under selection before demonstrating that  
72 population-level ASE can be detected with metagenomic and metatranscriptomic data collected  
73 by the *Tara* Oceans expedition<sup>42</sup> during its Arctic phase. Then we provided evidence of a  
74 quantitative link between ASE and natural selection.

## 75 **Material and Methods**

### 76 **Material sampling, mRNA extraction and transcriptome sequencing**

77 *Oithona similis* specimens were sampled at the North of the Large Bay of Toulon, France (Lat  
78 43°06' 02.3" N and Long 05°56' 53.4"E). Sampling took place in November 2016. The samples  
79 were collected from the upper water layers (0-10m) using zooplankton nets with a mesh of 90µm

80 and 200 $\mu$ m (0.5 m diameter and 2.5 m length). Samples were preserved in 70% ethanol and  
81 stored at -4°C. From the Large Bay of Toulon samples, *O. similis* individuals were isolated under  
82 the stereomicroscope. We selected two different development stages: four copepodites (juveniles)  
83 and four adult males. Each individual was transferred separately and crushed, with a tissue  
84 grinder (Axygen) into a 1.5 mL tube (Eppendorf). Total mRNAs were extracted using the ‘RNA  
85 isolation’ protocol from NucleoSpin RNA XS kit (Macherey-Nagel) and quantified on a Qubit  
86 2.0 with a RNA HS Assay kit (Invitrogen) and on a Bioanalyzer 2100 with a RNA 6000 Pico  
87 Assay kit (Agilent). cDNA were constructed using the SMARTer-Seq v4 Ultra low Input RNA  
88 kit (ClonTech). The libraries were constructed using the NEBNext Ultra II kit, and were  
89 sequenced with an Illumina HiSeq2500 (Supplementary Fig. 1).

#### 90 **Transcriptomes assembly and annotation**

91 Each read set was assembled with Trinity v2.5.1<sup>43</sup> using default parameters and transcripts were  
92 clustered using cd-hit v4.6.1<sup>44</sup> (Supplementary Table 1). To ensure the classification of the  
93 sampled individuals, each ribosomal read set were detected with SortMeRNA<sup>45</sup> and mapped with  
94 bwa v0.7.15 using default parameters<sup>46</sup> to 82 ribosomal 28S sequences of *Oithona* species used in  
95 Cornils et al., 2017 (Supplementary Fig. 2). The transcriptome assemblies were annotated with  
96 Transdecoder v5.1.0<sup>43</sup> to predict the open reading frames (ORFs) and protein sequences  
97 (Supplementary Table 1). In parallel, homology searches were also included as ORF retention  
98 criteria; the peptide sequences of the longest ORFs were aligned on *Oithona nana* proteome<sup>40</sup>  
99 using DIAMOND v0.9.22<sup>48</sup>. Protein domain annotation was performed on the final ORF  
100 predictions with Interproscan v5.17.56.0<sup>49</sup> and a threshold of e-value <10<sup>-5</sup> was applied for Pfam  
101 annotations. Finally, homology searches of the predicted proteins were done against the nr NCBI

102 database, restricted to Arthropoda (taxid: 6656), with DIAMOND v0.9.22 (Supplementary Fig.  
103 1).

#### 104 **Variant calling using *Tara* Oceans metagenomic and metatranscriptomic data**

105 We used metagenomic and metatranscriptomic reads generated from samples of the size fraction  
106 20–180  $\mu\text{m}$  collected in seven *Tara* Oceans stations TARA\_155, 158, 178, 206, 208, 209 and 210  
107 (Supplementary Table 2), according to protocols described in Alberti et al. 2017<sup>50</sup>.

108 The reference-free variant caller *DiscoSNP++*<sup>51,52</sup> was used to extract SNVs simultaneously  
109 from raw metagenomic and metatranscriptomic reads, and ran using parameters  $-b$  1. Only SNVs  
110 corresponding to biallelic loci with a minimum of 4x of depth of coverage in all stations were  
111 initially selected. Then, SNVs were clustered based on their loci co-abundance across samples  
112 using density-based clustering algorithm implemented in the R package *dbSCAN*<sup>53,54</sup> and ran with  
113 parameters  $\text{epsilon} = 10$  and  $\text{minPts} = 10$ . This generated three SNVs clusters, the largest of  
114 which contained 102,258 SNVs. To ensure the presence of *O. similis* SNVs without other  
115 species, we observed the fitting of the depth of coverage to the expected negative binomial  
116 distribution in each population (Supplementary Fig. 3). For each variant in each population, the  
117 B-allele frequency (BAF) and the population-level B-allele relative expression (BARE) were  
118 computed;  $BAF = \frac{G_B}{G_B + G_A}$  and  $BARE = \frac{T_B}{T_B + T_A}$ , with  $G_A$  and  $G_B$  the metagenomic read counts of  
119 the reference and alternative alleles respectively,  $T_A$  and  $T_B$  the metatranscriptomic read counts of  
120 the reference and alternative alleles respectively.

#### 121 **Variant filtering and annotation**

122 SNVs were filtered based on their metagenomic coverage. Those with a metagenomic coverage  
123 lying outside a threshold of  $\text{median} \pm 2 \sigma$  in at least one population, with a minimum and

124 maximum of 5x and 150x coverage were discarded. To keep out rare alleles and potential calling  
125 errors, only variants characterized by a BAF comprised between 0.9 and 0.1, and a BARE  
126 between 0.95 and 0.05 in at least one population were chosen for the final dataset resulting in  
127 25,768 SNVs (Supplementary Fig. 4).

128 The variant annotation was conducted in two steps. First, the variant sequences were relocated on  
129 the previously annotated *O.similis* transcripts using the “VCF\_creator.sh” program of  
130 *DiscoSNP++*. Secondly, a variant annotation was carried with SNPeff<sup>55</sup> to identify the location  
131 of variants within transcripts (i.e., exon or UTR) and to estimate their effect on the proteins  
132 (missense, synonymous or nonsense). The excess of candidate variant annotations was tested in  
133 the following classes: missenses, synonymous, 5' and 3'UTR. A significant excess was  
134 considered for a hypergeometric test p-value < 0.05.

### 135 **Genomic differentiation and detection of selection**

136 The differentiation among the seven populations was investigated through the computation of the  
137  $F_{ST}$  metric or Wright's fixation index<sup>56,57</sup>. For each locus, global  $F_{ST}$  including the seven  
138 populations and pairwise- $F_{ST}$  between each pair of population was computed, using the  
139 corresponding BAF matrix. For the global  $F_{ST}$  computation, a Hartigan's dip test for unimodality  
140 was performed<sup>58</sup>. We retained the median pairwise- $F_{ST}$  as a measure of the genomic  
141 differentiation between each population. The *pcadapt* R package v4.0.2<sup>59</sup> was used to detect  
142 selection among populations from the B-allele frequency matrix. The computation was run on  
143 “Pool-seq” mode, with a minimum allele frequency of 0.05 across the populations, and variants  
144 with a corrected Benjamini and Hochberg<sup>60</sup> p-value < 0.05 were considered under selection.

## 145 **Population-level ASE detection using metagenomic and metatranscriptomic data**

146 In each population, we first selected variants for  $BAF \neq \{0,1\}$ . Then, we computed  $D = BAF -$   
147  $BARE$ , as the deviation between the BAF and the BARE. In the absence of ASE,  $D$  is close to 0,  
148 as most of the biallelic loci are expected to have a balanced expression<sup>7,28,61</sup> we expect the  $D$   
149 distribution to follow a Gaussian distribution centered on 0. We estimated the Gaussian  
150 distribution parameters and tested the probability of a variant to belong to this distribution (“ $D$ -  
151 test” or “deviation test”). Given the large number of tests, we applied the Benjamini and  
152 Hochberg approach to control the False Discovery Rate (FDR).

153 We also computed a “low expression bias” test by comparing the read counts  $T_A$  and  $T_B$  to the  
154 observed metagenomic proportion  $1-BAF$  and  $BAF$  respectively with a chi-square test and  
155 applied the Benjamini and Hochberg correction for multiple testing. These two tests were applied  
156 to BAFs, BAREs and read counts of the seven populations separately and the seven sets of  
157 candidate loci targeted by ASE (deviation test q-value  $< 0.1$  and low expression bias test q-  
158 value  $< 0.1$ ) were crossed to identify loci under ASE in different populations, or shared ASEs.

159 To identify alleles targeted by both ASE and selection, the set of variants under ASE in each  
160 population was crossed with the set of loci detected under selection. The size of the intersection  
161 was tested by a hypergeometric test,  $Hypergeometric(q,m,n,k)$ , with  $q$  being number of alleles  
162 under ASE in the population and under selection (size of intersection),  $m$  being the total number  
163 of alleles under selection,  $n$  being the total number of variants under neutral evolution, and  $k$   
164 being the total number of alleles under ASE in the tested population. We considered that, in a  
165 given population, the number of alleles under both ASE and selection was significantly higher  
166 than expected by chance for p-value  $< 0.05$ .

## 167 **Gene enrichment analysis**

168 To identify specific biological function or processes associated to the variants, a domain-based  
169 analysis was conducted. The Pfam annotation of the transcripts carrying variants targeted by ASE  
170 and selection was used as entry for dcGO Enrichment<sup>62</sup>. A maximum of the best 300 GO-terms  
171 were chosen based on their z-score and FDR p-value ( $<10^{-3}$ ) in each ontology category. To  
172 reduce redundancy, these selected GO-terms were processed using REVIGO<sup>63</sup>, with a similarity  
173 parameter of 0.5 against the whole Uniprot catalogue under the SimRel algorithm. To complete  
174 the domain-based analysis, the functional annotations obtained from the homology searches  
175 against the nr were manually curated.

## 176 **Results**

### 177 ***Oithona similis* genomic differentiation and selection in Arctic Seas**

178 From metagenomic and metatranscriptomic raw data of seven sampling stations (Fig. 2a), we  
179 identified 25,768 expressed variants. Among them, 97% were relocated on *O. similis*  
180 transcriptomes.

181 The global distribution of  $F_{ST}$  of the seven populations was unimodal (Hartigans' dip test,  
182  $D=0.0012$ , p-value=0.99) with a median- $F_{ST}$  at 0.1, confirmed by the pairwise- $F_{ST}$  distributions  
183 (Supplementary Fig. 5). The seven populations were globally characterized by a weak to moderate  
184 differentiation, with a maximum median pairwise- $F_{ST}$  of 0.12 between populations from  
185 TARA\_210 and 155/178 (Fig. 2c,d). Populations from stations TARA\_158 (Norway Current),  
186 206 and 208 (Baffin Bay) were genetically closely-related, with the lowest median pairwise  $F_{ST}$   
187 (0.02), despite TARA\_158 did not co-geolocalize with the two other stations. The four other  
188 populations (TARA\_155, 178, 209, and 210) were equally distant from each other (0.1-0.12).

189 Finally, TARA\_158, 206 and 208 on one side, and TARA\_155, 178, 210 and 209 on the other  
190 side showed the same pattern of differentiation (0.05-0.07).

191 The PCA decomposed the genomic variability in six components; the first two components  
192 discriminated TARA\_155 and 178 from the others (32% and 28.1% variance explained  
193 respectively, Fig. 2b), and the third component differentiated TARA\_210 and 209 (19.5%). The  
194 fourth principal component separated TARA\_209 and 210 from 158/206/208 (11.3 %), with the  
195 last two concerning TARA\_158/206/208 (Supplementary Fig. 5). Globally, these results  
196 dovetailed with the  $F_{ST}$  analysis, with details discussed later. Finally, we detected 674 variants  
197 under selection, representing 2.6% of the dataset (corrected p-value < 0.05).

#### 198 **Loci targeted by population-level ASE and selection in Arctic populations**

199 The number of SNVs tested for ASE varied between 13,454 and 22,578 for TARA\_210 and 206  
200 respectively. As expected, the  $D$  deviation, representing the deviation between B-allele frequency  
201 and B-allele relative expression, followed a Gaussian distribution in each population (Fig. 3a and  
202 Supplementary Fig. 6). Variants under ASE (i.e. having a  $D$  significantly higher or lower than  
203 expected) were found in every population, ranging from 26 to 162 variants for TARA\_178 and  
204 206 respectively (Table 1). Overall, we found 587 variants under ASE, including 535 population-  
205 specific ASEs, and 52 ASEs shared by several populations (Fig.3b). Remarkably, 30 ASEs out of  
206 the 52 were present in the populations from TARA\_158, 206 and 208 that correspond to the  
207 genetically closest populations. The seven sets of variants under ASE were crossed with the set of  
208 variants under selection, as illustrated for TARA\_209 (Fig. 3c). The size of the intersection  
209 ranged from 5 to 42 variants (TARA\_155 and 210/206) and was significantly higher than  
210 expected by chance for all the populations (hypergeometric test p-value < 0.05). It represented a  
211 total of 152 unique variants under selection and ASE in at least one population (Table 1,

212 Supplementary Table 3), corresponding to 23% and 26% of variants under ASE and under  
213 selection respectively.

## 214 **Functional analysis of genes targeted by ASE and selection**

215 Among the 152 loci targeted by ASE and selection, 145 were relocated on *O. similis* transcripts  
216 (Supplementary Table 4). Amid these transcripts, 137 (90%) had a predicted ORF, 97 (64%)  
217 were linked to at least one Pfam domain and 90 (59%) to a functional annotation. Fifteen SNVs  
218 were missense variations, 59 synonymous, 31 and 29 were located in 5' and 3' UTR, without any  
219 significant excess (Supplementary Table 4 and 5). Based on homology searches (Supplementary  
220 Table 4), eight genes were linked to nervous system (Table2). Among them, two genes were  
221 involved in glutamate metabolism (omega-amidase NIT2 and 5-oxoprolinase), three were  
222 predicted to be glycine,  $\gamma$ -amino-butyric acid (GABA) and histamine neuroreceptors. Finally,  
223 four were also implicated in arthropods photoreceptors. The domain-based analysis confirmed  
224 these results, with an enrichment in GO-terms biological process also linked to nervous system  
225 (Supplementary Fig. 7).

## 226 **Discussion**

### 227 ***O. similis* populations are weakly structured within the Arctic Seas**

228 Global populations of *O. similis* are known to be composed of cryptic lineages<sup>47</sup>. Thus the  
229 assessment that the seven populations used in our study belong to the same *O. similis* cryptic  
230 lineage was a prerequisite for further analyses. The high proportion of variants mapped on the  
231 Mediterranean transcriptomes (97%) showed that the variant clustering method was efficient to  
232 regroup loci of an *O. similis* cryptic species. Plus, the unimodal distribution of  $F_{ST}$  showed that  
233 these populations of *O. similis* belong to the same polar cryptic species.

234 Secondly, we see that the seven populations examined are well connected with low median  
235 pairwise- $F_{ST}$ , despite the large distances separating them. Weak genetic structure in the polar  
236 region was already highlighted for other major Arctic copepods like *Calanus glacialis*<sup>64</sup>, and  
237 *Pseudocalanus* species<sup>65</sup>. The absence of structure was explained by ancient diminutions of  
238 effective population size due to past glaciations<sup>65-67</sup>, or high dispersal and connectivity between  
239 the present-day populations due to marine currents<sup>64</sup>.

240 Going into details, three different cases can be described. First, the differentiation of populations  
241 from TARA\_155 and 178 compared to the others could be explained by isolation-by-distance.  
242 Secondly, the geographically close populations from TARA\_210 and 209 present higher  
243 differentiation (median pairwise- $F_{ST}$  of 0.11). This could be explained by the West Greenland  
244 current acting as a physical barrier between the populations, which could lead to reduced gene  
245 flow<sup>68</sup>. At last, the strong link between TARA\_158 from Northern Atlantic current and  
246 TARA\_206/208 from the Baffin Bay is the most intriguing. Despite the large distances that  
247 separate the first one from the others, these three populations are well connected.

248 Metagenomic data enable to draw the silhouette of the population genetics but lacks resolution  
249 when dealing with intra-population structure. However, our findings are concordant with  
250 previous studies underpinning the large-scale dispersal, interconnectivity of marine zooplankton  
251 populations in other oceans, at diverse degrees<sup>38,69-71</sup>.

## 252 **Toward the link between ASE and natural selection**

253 Usually, at the individual level, the ASE analyses are achieved by measuring the difference in  
254 RNA-seq read counts of a heterozygous site. But at the population level, obtaining a large  
255 number of individuals remains a technical barrier especially for uncultured animals, or when the

256 amount of DNA retrieved from a single individual is not sufficient for high-throughput  
257 sequencing. Here, the detection of ASE at population level was possible by comparing the  
258 observed frequencies of the alleles based on metagenomic and metatranscriptomic data, which by  
259 passes the obstacles previously described.

260 In our study, the amount of detected ASE in each population was always lower than 1% of tested  
261 heterozygous variants, which altogether correspond to 2% of the total set of variants. In humans  
262 <sup>72</sup>, baboons <sup>21</sup> and flycatchers <sup>19</sup>, 17%, 23% of genes and 7.5% of transcripts were affected by  
263 ASE respectively. The difference with our results can be explained by one main reason. The  
264 detection of population-level ASE identifies only the ASE present in a large majority of  
265 individuals, which can be considered as “core ASEs”.

266 These core ASEs constitute the majority of detected ASEs and are population-specific, meaning  
267 the main drivers of this expression pattern are local conditions like different environmental  
268 pressures or population dynamics including, for example, the proportion of each developmental  
269 stage and sex, known to vary between populations and across seasons <sup>30,73</sup>. Another result is the  
270 presence of a small amount of variants affected by ASE in different populations. Most of these  
271 variants are under ASE in at least two of the three closest populations from TARA\_158, 206 and  
272 208. First, the genetic closeness and large geographic distances between these three populations  
273 suggest that their shared ASEs are under an environmental independent genetic control.  
274 Secondly, the number of variants tested for ASE is higher in these three populations than the  
275 others, leading to a greater proportion of ASEs detected which also elevates the chances for a  
276 variant to be declared under ASE in several populations.

277 A significant amount of SNVs (152) were subject to selection among the seven populations and  
278 to ASE in at least one population. We confirmed our first hypothesis (Fig. 1), as exemplified with  
279 the variant 841109 (Fig. 3d), characterized by an ASE in favor of the B-allele in TARA\_209 and  
280 fixation of this allele in TARA\_210. Three main features of ASE can be under selection. First,  
281 the observed variant can be in linkage with another variation in upstream *cis*-regulatory elements  
282 like transcription factors fixation sites, or epialleles<sup>7</sup>. Secondly, the annotation of candidate  
283 variants with SNPeff revealed a majority of variants located in 5' and 3'UTRs, which are  
284 variations known to both affect transcription efficiency through mRNA secondary structures,  
285 stability and location<sup>74-76</sup>. For variants located in exons, a majority were identified as  
286 synonymous mutations, growingly described as potential target of selection by codon usage bias,  
287 codon context, mRNA secondary structure or transcription and translation dynamics<sup>77,78</sup>. Finally,  
288 fifteen missense mutations were spotted, but with moderate predicted impact on protein amino  
289 acid composition. However, we did not find premature nonsense mutation, even if variants under  
290 ASE has been described to trigger or escape potential nonsense-mediated decay<sup>28,61,79</sup>, but the  
291 possibility that the causal variation is located in introns cannot be ruled out.

292 The process of adaptation through gene expression was suspected in human populations and  
293 investigated thanks to the large and accessible amount of data. In a first study, a link has been  
294 established between gene expression and selection, affecting particular genes and phenotypes,  
295 looking at *cis*-acting SNPs<sup>80</sup>. In a second study, the team was able to detect ASE in different  
296 populations and to quantify genetic differentiation and selection<sup>61</sup>. They found particularly one  
297 gene that shows strong differentiation between European and African populations and under ASE  
298 in Europeans and not in Africans. However, they did not quantify this phenomenon. Both  
299 emphasized the impact of selection on gene expression. In the same way, another approach

300 showed that ASE or expression variations with high effect size were rare in the populations,  
301 based on intra-population analyses in *Capsella grandiflora* and human<sup>28,81</sup>. This situation is  
302 presumably encountered in our analysis, as exemplified with the B-allele of variant 20760212,  
303 under ASE and with a low genomic frequency in TARA\_210, but fixed in the others (Fig. 3d).  
304 Our results complete previous analyses, as they quantify the link between ASE and selection in  
305 populations and reveal the evolutive potency of ASE, for the first time at the population-level. It  
306 remains to understand the nature of the association between ASE and selection. To address this  
307 question, we formulate the hypothesis that they impact chronologically the same loci, following  
308 constant or increasing selective pressure as well as environmental changes (Fig. 4).

309 **Nervous system and visual perception are important targets of the natural selection and**  
310 **ASE in *O. similis***

311 This evolutive link between ASE and selection is supported by the biological functions associated  
312 to the targeted genes, which are involved notably in the copepods nervous system in two ways.  
313 The first result is the presence of genes implicated in glutamate metabolism and glycine and/or  
314 GABA receptors. Glutamate and GABA are respectively excitatory and inhibitory  
315 neurotransmitters in arthropods motor neurons<sup>82</sup>. Plus, glycine and GABA receptors have  
316 already been described as a target of selection in *O. nana* in Mediterranean Sea<sup>40,41</sup>. Secondly, the  
317 functional analysis revealed also the importance of the eye and visual perception in the *O. similis*  
318 evolution.

319 Copepod nervous system constitutes a key trait for its reproduction and survival, and based on  
320 our data, a prime target for evolution, allowing higher capacity of perceiving and fast reacting  
321 leading to more efficient predator escape, prey catching and mating. This can explain the great  
322 evolutive success of these animals<sup>35,83,84</sup>.

## 323 **Conclusion**

324 Gene expression variation is thought to play a crucial role in evolutive and adaptive history of  
325 natural populations. Herein, we developed proper methods integrating metagenomic and  
326 metatranscriptomic data to detect ASE at the population-level for the first time. Then, we  
327 demonstrated the link between ASE and natural selection by providing a quantitative observation  
328 of this phenomenon and its impact on specific biological features of copepods. In the future, we  
329 will try to generalize these observations to other organisms. Then, we will understand the nature  
330 of the link between ASE and natural selection by questioning the chronology between the two  
331 mechanisms.

## 332 **Acknowledgments**

333 We thank the people and sponsors who participated in the *Tara* Oceans Expedition 2009–2013:  
334 Centre National de la Recherche Scientifique, European Molecular Biology Laboratory,  
335 Genoscope/Commissariat à l’Energie Atomique, the French Government “Investissements  
336 d’Avenir” programmes OCEANOMICS (ANR-11- BTBR-0008), FRANCE GENOMIQUE  
337 (ANR-10-INBS-09-08), Agnes b., the Veolia Environment Foundation, Region Bretagne, World  
338 Courier, Illumina, Cap L’Orient, the Electricite de France (EDF) Foundation EDF Diversiterre,  
339 Fondation pour la Recherche sur la Biodiversite, the Prince Albert II de Monaco Foundation,  
340 Etienne Bourgois and the *Tara* schooner and its captain and crew. *Tara* Oceans would not exist  
341 without continuous support from 23 institutes ([oceans.tara-expeditions.org](http://oceans.tara-expeditions.org)). This is contribution  
342 number XX from *Tara* Oceans.

## 343 **Author's contributions**

344 Individuals for transcriptome production were sampled by J-LJ and KS. KS extracted RNA, EP  
345 and KL prepared the libraries and sequencing, MAM assembled the reads and RLJ annotated  
346 transcriptomes. PP and CA gave expertise support on *DiscoSNP++* and statistical framework  
347 respectively. RLJ and MAM performed the analyses and wrote the manuscript. MAM designed  
348 and supervised the study. J-LJ and PW offered scientific support.

## 349 **Competing interests**

350 The authors declare no competing interests.

## 351 **References**

- 352 1. Szabo, P. E. & Mann, J. R. Allele-specific expression and total expression levels of  
353 imprinted genes during early mouse development: implications for imprinting mechanism.  
354 *Genes Dev.* **9**, 3097–3108 (1995).
- 355 2. Wei, X. & Wang, X. A computational workflow to identify allele-specific expression and  
356 epigenetic modification in maize. *Genomics, Proteomics Bioinforma.* **11**, 247–252 (2013).
- 357 3. Ginart, P. *et al.* Visualizing allele-specific expression in single cells reveals epigenetic  
358 mosaicism in an H19loss-of-imprinting mutant. *Genes Dev.* **30**, 567–578 (2016).
- 359 4. Lonsdale, Z. *et al.* Allele specific expression and methylation in the bumblebee, *Bombus*  
360 *terrestris*. *PeerJ* **5**, e3798 (2017).
- 361 5. Bailey, S. D., Virtanen, C., Haibe-Kains, B. & Lupien, M. ABC: A tool to identify SNVs  
362 causing allele-specific transcription factor binding from ChIP-Seq experiments.  
363 *Bioinformatics* **31**, 3057–3059 (2015).
- 364 6. Cavalli, M. *et al.* Allele-specific transcription factor binding to common and rare variants  
365 associated with disease and gene expression. *Hum. Genet.* **135**, 485–497 (2016).
- 366 7. Castel, S. E., Levy-Moonshine, A., Mohammadi, P., Banks, E. & Lappalainen, T. Tools  
367 and best practices for data processing in allelic expression analysis. *Genome Biol.* **16**, 195  
368 (2015).
- 369 8. Rivas, M. A. *et al.* Impact of predicted protein-truncating genetic variants on the human

- 370 transcriptome. *Science* (80-. ). **348**, 666–669 (2015).
- 371 9. Pirinen, M. *et al.* Assessing allele-specific expression across multiple tissues from RNA-  
372 seq read data. *Bioinformatics* **31**, 2497–2504 (2015).
- 373 10. Lu, R. *et al.* Analyzing allele specific RNA expression using mixture models. *BMC*  
374 *Genomics* **16**, 566 (2015).
- 375 11. Harvey, C. T. *et al.* QuASAR: Quantitative allele-specific analysis of reads.  
376 *Bioinformatics* **31**, 1235–1242 (2015).
- 377 12. Miao, Z., Alvarez, M., Pajukanta, P. & Ko, A. ASElux: An ultra-fast and accurate allelic  
378 reads counter. *Bioinformatics* **34**, 1313–1320 (2018).
- 379 13. Mayba, O. *et al.* MBASED: allele-specific expression detection in cancer tissues and cell  
380 lines. *Genome Biol.* **15**, 405 (2014).
- 381 14. Skelly, D. A., Johansson, M., Madeoy, J., Wakefield, J. & Akey, J. M. A powerful and  
382 flexible statistical framework for testing hypotheses of allele-specific gene expression  
383 from RNA-seq data. *Genome Res.* **21**, 1728–1737 (2011).
- 384 15. M. Dong, Y. J. Single-Cell Allele-Specific Gene Expression Analysis. *Comput. Methods*  
385 *Single-Cell Data Anal.* **1935**, (2019).
- 386 16. Ge, B. *et al.* Global patterns of cis variation in human cells revealed by high-density allelic  
387 expression analysis. *Nat. Genet.* **41**, 1216–1222 (2009).
- 388 17. Signor, S. A. & Nuzhdin, S. V. The Evolution of Gene Expression in cis and trans. *Trends*  
389 *Genet.* 1–13 (2018). doi:10.1016/j.tig.2018.03.007
- 390 18. McKean, D. M. *et al.* Loss of RNA expression and allele-specific expression associated  
391 with congenital heart disease. *Nat. Commun.* **7**, 1–9 (2016).
- 392 19. Wang, M., Uebbing, S. & Ellegren, H. Bayesian inference of allele-specific gene  
393 expression indicates abundant Cis-regulatory variation in natural flycatcher populations.  
394 *Genome Biol. Evol.* **9**, 1266–1279 (2017).
- 395 20. Howe, B., Umrigar, A. & Tsien, F. Chromosome Preparation From Cultured Cells. *J. Vis.*  
396 *Exp.* 3–7 (2014). doi:10.3791/50203
- 397 21. J. Tung, M. Y. Akinyi, S. Mutura, J. Altmann, G. A. W. and S. C. & Alberts. Allele-  
398 specific gene expression in a wild nonhuman primate population. *Mol. Ecol.* **2**, 147–185  
399 (2015).
- 400 22. Buil, A. *et al.* Gene-gene and gene-environment interactions detected by transcriptome  
401 sequence analysis in twins. *Nat. Genet.* **47**, 88–91 (2014).
- 402 23. Cheung, V. G. *et al.* Monozygotic Twins Reveal Germline Contribution to Allelic  
403 Expression Differences. *Am. J. Hum. Genet.* **82**, 1357–1360 (2008).
- 404 24. Moyerbrailean, G. A. *et al.* High-throughput allele-specific expression across 250

- 405 environmental conditions. *Genome Res.* **26**, 1627–1638 (2016).
- 406 25. Knowles, D. A. *et al.* Allele-specific expression reveals interactions between genetic  
407 variation and environment. *Nat. Methods* **14**, 699–702 (2017).
- 408 26. Leon-Novelo, L., Gerken, A. R., Graze, R. M., McIntyre, L. M. & Marroni, F. Direct  
409 Testing for Allele-Specific Expression Differences Between Conditions. *G3 GENES,*  
410 *GENOMES, Genet.* **8**, g3.300139.2017 (2017).
- 411 27. Jensen, J. D. *et al.* The importance of the neutral theory in 1968 and 50 years on: a  
412 response to Kern & Hahn 2018. *Evolution (N. Y).* 1968–1971 (2018).  
413 doi:10.1111/evo.13650
- 414 28. Lappalainen, T. *et al.* Transcriptome and genome sequencing uncovers functional variation  
415 in humans. *Nature* **501**, 506–511 (2013).
- 416 29. Claus, C. Die Copepoden-Fauna von Nizza. Ein Beitrag zur Charakteristik der Formen und  
417 deren Abänderungen ‘im Sinna Darwin’s’. *Elwebt’sche Univ. Marbg. Leipzig* **1**, 1:34  
418 (1866).
- 419 30. Dvoretzky, V. G. Seasonal mortality rates of *Oithona similis* (Cyclopoida) in a large Arctic  
420 fjord. *Polar Sci.* **6**, 263–269 (2012).
- 421 31. Castellani. Contribution to the Themed Section□: ‘ The Role of Zooplankton in Marine  
422 Biogeochemical Cycles□: From Fine Scale to Global Marine zooplankton and the  
423 Metabolic Theory of Ecology□: is it a predictive tool□? *J. Plankton Res.* **38**, 762–770  
424 (2016).
- 425 32. Blachowiak-Samolyk, K., Kwasniewski, S., Hop, H. & Falk-Petersen, S. Magnitude of  
426 mesozooplankton variability: A case study from the Marginal Ice Zone of the Barents Sea  
427 in spring. *J. Plankton Res.* **30**, 311–323 (2008).
- 428 33. Zamora-Terol, S., Nielsen, T. G. & Saiz, E. Plankton community structure and role of  
429 *Oithona similis* on the western coast of Greenland during the winter-spring transition. *Mar.*  
430 *Ecol. Prog. Ser.* **483**, 85–102 (2013).
- 431 34. Humes, A. G. How Many Copepods? *Hydrobiologia* **293**, 1–7 (1994).
- 432 35. Kjørboe, T. What makes pelagic copepods so successful? *J. Plankton Res.* **33**, 677–685  
433 (2011).
- 434 36. Gallienne, C. P. Is *Oithona* the most important copepod in the world’s oceans? *J. Plankton*  
435 *Res.* **23**, 1421–1432 (2001).
- 436 37. Wassmann, P. *et al.* Food webs and carbon flux in the Barents Sea. *Prog. Oceanogr.* **71**,  
437 232–287 (2006).
- 438 38. Peijnenburg, K. T. C. A. & Goetze, E. High evolutionary potential of marine zooplankton.  
439 *Ecol. Evol.* **3**, 2765–2781 (2013).
- 440 39. Riginos, C., Crandall, E. D., Liggins, L., Bongaerts, P. & Treml, E. A. Navigating the

- 441 currents of seascape genomics: How spatial analyses can augment population genomic  
442 studies. *Curr. Zool.* **62**, 581–601 (2016).
- 443 40. Madoui, M. A. *et al.* New insights into global biogeography, population structure and  
444 natural selection from the genome of the epipelagic copepod *Oithona*. *Mol. Ecol.* **26**,  
445 4467–4482 (2017).
- 446 41. Arif, M. *et al.* Discovering Millions of Plankton Genomic Markers from the Atlantic  
447 Ocean and the Mediterranean Sea. *Mol. Ecol. Resour.* 0–3 (2018). doi:10.1111/1755-  
448 0998.12985
- 449 42. Karsenti, E. *et al.* A Holistic Approach to Marine Eco-Systems Biology. *PLoS Biol.* **9**,  
450 e1001177 (2011).
- 451 43. Haas, B. J. *et al.* De novo transcript sequence reconstruction from RNA-seq using the  
452 Trinity platform for reference generation and analysis. *Nat. Protoc.* **8**, 1494–1512 (2013).
- 453 44. Fu, L., Niu, B., Zhu, Z., Wu, S. & Li, W. CD-HIT: Accelerated for clustering the next-  
454 generation sequencing data. *Bioinformatics* **28**, 3150–3152 (2012).
- 455 45. Kopylova, E., Noé, L. & Touzet, H. SortMeRNA: Fast and accurate filtering of ribosomal  
456 RNAs in metatranscriptomic data. *Bioinformatics* **28**, 3211–3217 (2012).
- 457 46. Li, H. & Durbin, R. Fast and accurate long-read alignment with Burrows-Wheeler  
458 transform. *Bioinformatics* **26**, 589–595 (2009).
- 459 47. Cornils, A., Wend-Heckmann, B. & Held, C. Global phylogeography of *Oithona similis*  
460 s.l. (Crustacea, Copepoda, Oithonidae) – A cosmopolitan plankton species or a complex of  
461 cryptic lineages? *Mol. Phylogenet. Evol.* **107**, 473–485 (2017).
- 462 48. Buchfink, B., Xie, C. & Huson, D. H. Fast and sensitive protein alignment using  
463 DIAMOND. *Nat. Methods* **12**, 59–60 (2014).
- 464 49. Jones, P. *et al.* InterProScan 5: genome-scale protein function classification.  
465 *Bioinformatics* **30**, 1236–1240 (2014).
- 466 50. Alberti, A. *et al.* Viral to metazoan marine plankton nucleotide sequences from the Tara  
467 Oceans expedition. *Sci. Data* **4**, 170093 (2017).
- 468 51. Uricaru, R. *et al.* Reference-free detection of isolated SNPs. *Nucleic Acids Res.* (2014).  
469 doi:10.1093/nar/gku1187
- 470 52. Peterlongo, P., Riou, C., Drezen, E. & Lemaitre, C. DiscoSnp++: de novo detection of  
471 small variants from raw unassembled read set(s). *bioRxiv* 209965 (2017).  
472 doi:10.1101/209965
- 473 53. Ester, M., Kriegel, H.-P., Sander, J. & Xu, X. *A Density-Based Algorithm for Discovering*  
474 *Clusters in Large Spatial Databases with Noise.* (1996).
- 475 54. Ram, A., Jalal, S., Jalal, A. S. & Kumar, M. A Density Based Algorithm for Discovering  
476 Density Varied Clusters in Large Spatial Databases. *Int. J. Comput. Appl.* **3**, 1–4 (2010).

- 477 55. Cingolani, P. and Platts, A. and Coon, M. and Nguyen, T. and Wang, L. and Land, S.J. and  
478 Lu, X. and Ruden, D. M. A program for annotating and predicting the effects of single  
479 nucleotide polymorphisms, SnpEff: SNPs in the genome of *Drosophila melanogaster* strain  
480 w1118□; iso-2; iso-3. *Fly* **6**, 80–92 (2012).
- 481 56. B. S. Weir and C. Clark Cockerham. Estimating F-Statistics for the Analysis of Population  
482 Structure. *Evolution (N. Y.)* **38**, 1358–1370 (1984).
- 483 57. Wright, S. the Genetical Structure of Populations. *Ann. Eugen.* **15**, 323–354 (1951).
- 484 58. Hartigan, J. A. & Hartigan, P. M. The dip test of unimodality. *Ann. Stat.* **13**, 70–84 (1985).
- 485 59. Luu, K., Bazin, E. & Blum, M. G. B. pcadapt: an R package to perform genome scans for  
486 selection based on principal component analysis. *Mol. Ecol. Resour.* **17**, 67–77 (2017).
- 487 60. Benjamini, Y. & Hochberg, Y. Controlling the False Discovery Rate□: A Practical and  
488 Powerful Approach to Multiple Testing. *J. R. Stat. Soc. Ser. B* **57**, 289–300 (1995).
- 489 61. Tian, L. *et al.* Genome-wide comparison of allele-specific gene expression between  
490 African and European populations. *Hum. Mol. Genet.* **27**, 1067–1077 (2018).
- 491 62. Fang, H. & Gough, J. DcGO: Database of domain-centric ontologies on functions,  
492 phenotypes, diseases and more. *Nucleic Acids Res.* **41**, (2013).
- 493 63. Supek, F., Bošnjak, M., Škunca, N. & Šmuc, T. Revigo summarizes and visualizes long  
494 lists of gene ontology terms. *PLoS One* **6**, (2011).
- 495 64. Weydmann, A., Coelho, N. C., Serrão, E. A., Burzyński, A. & Pearson, G. A. Pan-Arctic  
496 population of the keystone copepod *Calanus glacialis*. *Polar Biol.* **39**, 2311–2318 (2016).
- 497 65. Aarbakke, O. N. S., Bucklin, A., Halsband, C. & Norrbin, F. Comparative phylogeography  
498 and demographic history of five sibling species of *Pseudocalanus* (Copepoda: Calanoida)  
499 in the North Atlantic Ocean. *J. Exp. Mar. Bio. Ecol.* **461**, 479–488 (2014).
- 500 66. Edmands, S. Phylogeography of the intertidal copepod *Tigriopus californicus* reveals  
501 substantially reduced population differentiation at northern latitudes. *Mol. Ecol.* **10**, 1743–  
502 1750 (2001).
- 503 67. Bucklin, A. & Wiebe, P. H. Low mitochondrial diversity and small effective population  
504 sizes of the copepods *Calanus finmarchicus* and *Nannocalanus minor*: Possible impact of  
505 climatic variation during recent glaciation. *J. Hered.* **89**, 383–392 (1998).
- 506 68. Myers, P. G., Donnelly, C. & Ribergaard, M. H. Structure and variability of the West  
507 Greenland Current in Summer derived from 6 repeat standard sections. *Prog. Oceanogr.*  
508 (2008). doi:10.1016/j.pocean.2008.12.003
- 509 69. Blanco-Bercial, L. & Bucklin, A. New view of population genetics of zooplankton: RAD-  
510 seq analysis reveals population structure of the North Atlantic planktonic copepod  
511 *Centropages typicus*. *Mol. Ecol.* **25**, 1566–1580 (2016).
- 512 70. Höring, F., Cornils, A., Auel, H., Bode, M. & Held, C. Population genetic structure of

- 513 Calanoides natalis (Copepoda, Calanoida) in the eastern Atlantic Ocean and Benguela  
514 upwelling system. *J. Plankton Res.* **39**, 618–630 (2017).
- 515 71. Goetze, E. Global Population Genetic Structure and Biogeography of the Oceanic  
516 Copepods Eucalanus Hyalinus and E. Spinifer. *Evolution (N. Y.)*. **59**, 2378 (2005).
- 517 72. Zhang, S. *et al.* Genome-wide identification of allele-specific effects on gene expression  
518 for single and multiple individuals. *Gene* **533**, 366–373 (2014).
- 519 73. Lischka, S. & Hagen, W. Life histories of the copepods Pseudocalanus minutus, P. acuspes  
520 (Calanoida) and Oithona similis (Cyclopoida) in the Arctic Kongsfjorden (Svalbard).  
521 *Polar Biol.* **28**, 910–921 (2005).
- 522 74. Mignone, F., Gissi, C., Liuni, S., Pesole, G. & others. Untranslated regions of mRNAs.  
523 *Genome Biol* **3**, 4–1 (2002).
- 524 75. Dvir, S. *et al.* Deciphering the rules by which 5'-UTR sequences affect protein expression  
525 in yeast. *Proc. Natl. Acad. Sci.* **110**, E2792–E2801 (2013).
- 526 76. Matoulkova, E., Michalova, E., Vojtesek, B. & Hrstka, R. The role of the 3' untranslated  
527 region in post-transcriptional regulation of protein expression in mammalian cells. *RNA*  
528 *Biol.* **9**, 563–576 (2012).
- 529 77. Shabalina, S. A., Spiridonov, N. A. & Kashina, A. Sounds of silence: Synonymous  
530 nucleotides as a key to biological regulation and complexity. *Nucleic Acids Res.* **41**, 2073–  
531 2094 (2013).
- 532 78. Ingvarsson, P. K. Natural Selection on Synonymous and Nonsynonymous Mutations  
533 Shapes Patterns of Polymorphism in Populus tremula. *Mol. Biol. Evol.* **27**, 650–660  
534 (2010).
- 535 79. Rivas, M. A. *et al.* Effect of predicted protein-truncating genetic variants on the human  
536 transcriptome. *Science (80-. )*. **348**, 666–669 (2015).
- 537 80. Fraser, H. B. Gene expression drives local adaptation in humans Gene expression drives  
538 local adaptation in humans. *Genome Res.* 1089–1096 (2013). doi:10.1101/gr.152710.112
- 539 81. Josephs, E. B., Lee, Y. W., Stinchcombe, J. R. & Wright, S. I. Association mapping  
540 reveals the role of purifying selection in the maintenance of genomic variation in gene  
541 expression. *Proc. Natl. Acad. Sci.* **112**, 15390–15395 (2015).
- 542 82. Smarandache-Wellmann, C. R. Arthropod neurons and nervous system. *Curr. Biol.* **26**,  
543 R960–R965 (2016).
- 544 83. Svensen, C. Remote prey detection in Oithona similis: hydromechanical versus chemical  
545 cues. *J. Plankton Res.* **22**, 1155–1166 (2000).
- 546 84. Kiørboe, T., Andersen, A., Langlois, V. J. & Jakobsen, H. H. Unsteady motion: Escape  
547 jumps in planktonic copepods, their kinematics and energetics. *J. R. Soc. Interface* **7**,  
548 1591–1602 (2010).

- 549 85. Denno, M. E., Privman, E., Borman, R., Wolin, D. & Venton, B. J. Quantification of  
550 histamine and carcinine in *Drosophila melanogaster* tissues. *ACS Chem Neurosci* **7**, 407–  
551 414 (2016).
- 552 86. Monastirioti, M. Biogenic amine systems in the fruit fly *Drosophila melanogaster*.  
553 *Microsc. Res. Tech.* **45**, 106–121 (1999).
- 554 87. Stuart, A. E. From fruit flies to barnacles, histamine is the neurotransmitter of arthropod  
555 photoreceptors. *Neuron* **22**, 431–433 (1999).
- 556 88. Gurudev, N., Yuan, M. & Knust, E. chaoptin, prominin, eyes shut and crumbs form a  
557 genetic network controlling the apical compartment of *Drosophila* photoreceptor cells.  
558 *Biol. Open* **3**, 332–341 (2014).
- 559 89. Krantz, D. E. & Zipursky, S. L. *Drosophila* chaoptin, a member of the leucine-rich repeat  
560 family, is a photoreceptor cell-specific adhesion molecule. *EMBO J.* **9**, 1969–77 (1990).
- 561 90. Masai, I., Okazaki, A., Hosoyat, T. & Hottatt, Y. *Drosophila* retinal degeneration A gene  
562 encodes an eye-specific diacylglycerol kinase with cysteine-rich zinc-finger motifs and  
563 ankyrin repeats (signal transduction/phosphatidylinositol metabolism). *Neurobiology* **90**,  
564 11157–11161 (1993).
- 565 91. Wang, T. & Montell, C. Phototransduction and retinal degeneration in *Drosophila*.  
566 *Pflugers Arch. Eur. J. Physiol.* **454**, 821–847 (2007).
- 567 92. Rawls, A. S. Strabismus requires Flamingo and Prickle function to regulate tissue polarity  
568 in the *Drosophila* eye. *Development* **130**, 1877–1887 (2003).
- 569 93. Leung, V. *et al.* The planar cell polarity protein Vangl2 is required for retinal axon  
570 guidance. *Dev. Neurobiol.* **76**, 150–165 (2016).

571

## 572 **Tables**

573 **Table 1:** Allele-specific expression detection and link with selection by population

574 **Table 2:** Functional annotations of variants targeted by ASE and selection implicated in nervous  
575 system

576 **Supplementary Table 1:** *Oithona similis* Mediterranean transcriptomes summary

577 **Supplementary Table 2:** *Tara* Oceans and *Oithona similis* Mediterranean transcriptomes  
578 samples accession numbers

579 **Supplementary Table 3:** Variants targeted by ASE and selection statistics

580 **Supplementary Table 4:** Variants targeted by ASE and selection functional annotations

581 **Supplementary Table 5:** Variant annotation by SNPeff

582 **Figures**

583 **Figure 1:** Population genomic and transcriptomic profiles of a biallelic locus in a case of **a**,  
584 Neutral evolution and balanced expression; **b**, Selection in favor of the B-allele; **c**, ASE in favor  
585 of the B-allele.

586 **Figure 2:** Genomic differentiation of *O. similis* populations from Arctic Seas. **a**, Geographic  
587 locations of the seven *Tara* Oceans sampling sites: Northern Atlantic (blue), Kara Sea (green),  
588 Baffin Bay (orange) and Labrador Sea (grey). **b**, Principal Component Analysis (PCA) computed  
589 by *pcadapt* based on allele frequencies. **c**, Pairwise- $F_{ST}$  matrix. The median (mean) of each  
590 pairwise- $F_{ST}$  distribution computed on allele frequencies is indicated. **d**, Graph representing the  
591 genomic differentiation of the seven populations of *O. similis*. The nodes represent the  
592 populations; their width reflects their centrality in the graph. The edges correspond to the genetic  
593 relatedness based on the median pairwise- $F_{ST}$  between each pair of population; 0.02 (large solid  
594 line), 0.05 to 0.07 (thin solid line) and 0.11 to 0.12 (dashed line).

595 **Figure 3:** Population Allele-specific expression detection and link with natural selection. **a**, The  
596 deviation  $D$  distribution in TARA\_209. The red line corresponds to the Gaussian distribution  
597 estimated from the data. **b**, Upset plot of the ASE detection in the seven populations. Each bar of  
598 the upper plot corresponds to the number of variants under ASE in the population(s) indicated by  
599 black dots in the lower plot. **c**, Crossing ASE and selection. The yellow circle represents the total  
600 set of variants. In green, the number of heterozygous variants tested for ASE in TARA\_209. In  
601 blue and red, the amount of detected variants under ASE in TARA\_209 and under selection  
602 among the populations respectively. In purple, the intersection comprising variants under ASE in  
603 TARA\_209 and under selection, with its hypergeometric test p-value. **d**, Metagenomic and  
604 metatranscriptomic profiles of variants 841109 and 20760212. Each population is indicated on  
605 the x-axis, with the associated B-allele frequency (red) and B-allele relative expression (blue).  
606 The frequency is shown on the y-axis. The asterisks mean ASE was detected in the corresponding  
607 population.

608 **Figure 4:** From Allele-specific expression to natural selection. **a**, Evolution of allele frequency  
609 and allele relative expression over time. **b**, Evolution of selective pressure over time

610 **Supplementary Fig 1:** Method pipeline overview

611 **Supplementary Fig 2:** Validation of taxonomic assignment

612 **Supplementary Fig 3:** *Oithona similis* depth of coverage of biallelic loci in seven *Tara* Oceans  
613 samples

- 614 **Supplementary Fig 4:** Metagenomic coverage distribution of the seven *Tara* Oceans samples
- 615 **Supplementary Fig 5:** Genomic differentiation of Arctic Seas *Oithona similis* populations
- 616 **Supplementary Fig 6:** Allele-specific expression detection
- 617 **Supplementary Fig 7:** Functional analysis of *O. similis* transcripts targeted by ASE and  
618 selection
- 619
- 620

621 **Table 1:** Allele-specific expression detection and link with selection by population

Population	Genomic median depth of coverage	Number of tested variants	Number of variants under ASE	Number of variants under ASE and selection	Hypergeometric test p-value
TARA_155	25	18,812	91	6	9.89E-3*
TARA_158	35	21,476	131	29	5.06E-20*
TARA_178	24	18,145	26	9	5E-11*
TARA_206	55	22,578	162	42	4.82E-31*
TARA_208	48	21,469	133	14	2.2E-6*
TARA_209	12	13,956	62	24	1.05E-23*
TARA_210	14	13,454	69	42	8.89E-51*
Overall	-	25,768	587 (2.3%)	152 (0.59%)	-

622

623

624

625 **Table 2:** Functional annotations of variants targeted by ASE and selection implicated in nervous system

VarID	Ref	Alt	Homology search	Pfam	SnpEff Localization	SnpEff Impact	References
722267	A	G	histamine H1 receptor	PF00001	3' UTR	MODIFIER	85-87
9665345	T	G	chaoptin	PF13306   PF13855	synonymous variant	LOW	88,89
15623788	G	A	eye-specific diacylglycerol kinase	PF13637	synonymous variant	LOW	90,91
23795359	A	T	vang-like protein 2-B	PF06638	synonymous variant	LOW	92,93
1276227	C	T	glycine receptor subunit alpha-2 / gamma-aminobutyric acid receptor subunit alpha-6	PF02932   PF2931	3' UTR	MODIFIER	-
1404415	G	C	omega-amidase NIT2	PF00795	3' UTR	MODIFIER	-
11174785	A	G	5-oxoprolinase	PF02538   PF05378   PF01968	5' UTR	MODIFIER	-
11690229	A	T	glycine receptor subunit alpha-2	PF02931	synonymous variant	LOW	-

626

627

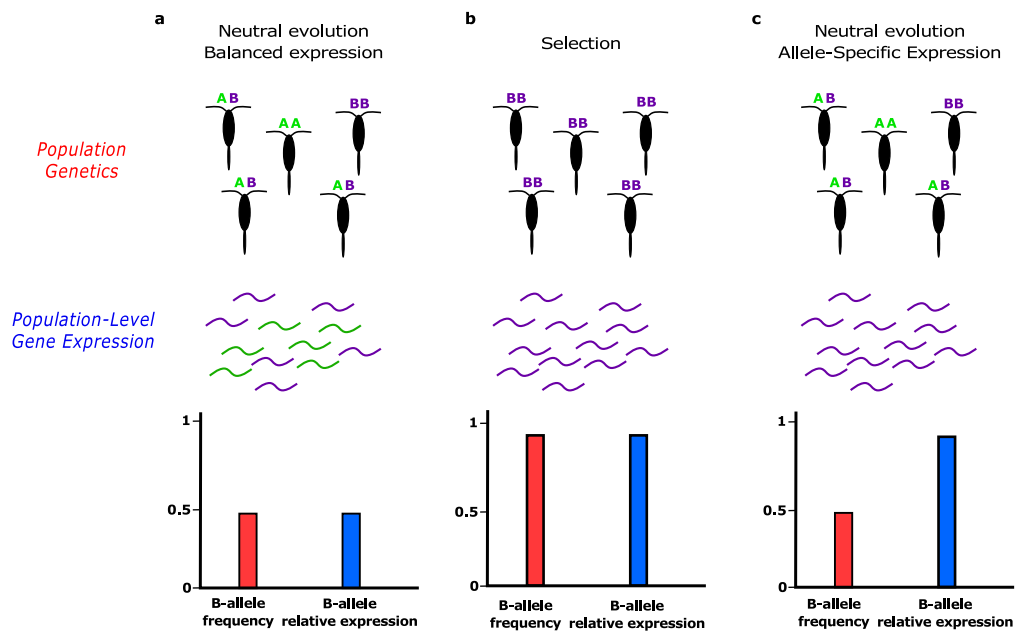


Figure 1: Population genomic and transcriptomic profiles of a biallelic locus in a case of **a**, Neutral evolution and balanced expression; **b**, Selection in favor of the B-allele; **c**, ASE in favor of the B-allele.

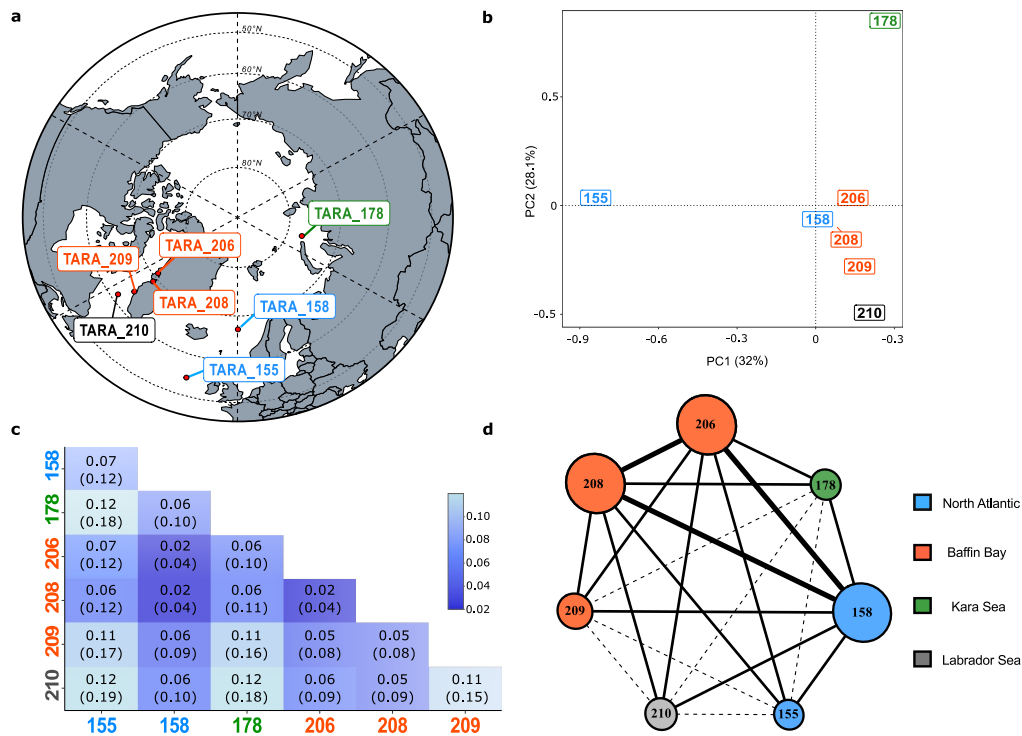


Figure 2: Genomic differentiation of *O. similis* populations from Arctic Seas. **a**, Geographic locations of the seven *Tara* Oceans sampling sites: Northern Atlantic (blue), Kara Sea (green), Baffin Bay (orange) and Labrador Sea (grey). **b**, Principal Component Analysis (PCA) computed by *pcadapt* based on allele frequencies. **c**, Pairwise- $F_{ST}$  matrix. The median (mean) of each pairwise- $F_{ST}$  distribution computed on allele frequencies is indicated. **d**, Graph representing the genomic differentiation of the seven populations of *O. similis*. The nodes represent the populations; their width reflects their centrality in the graph. The edges correspond to the genetic relatedness based on the median pairwise- $F_{ST}$  between each pair of population; 0.02 (large solid line), 0.05 to 0.07 (thin solid line) and 0.11 to 0.12 (dashed line).

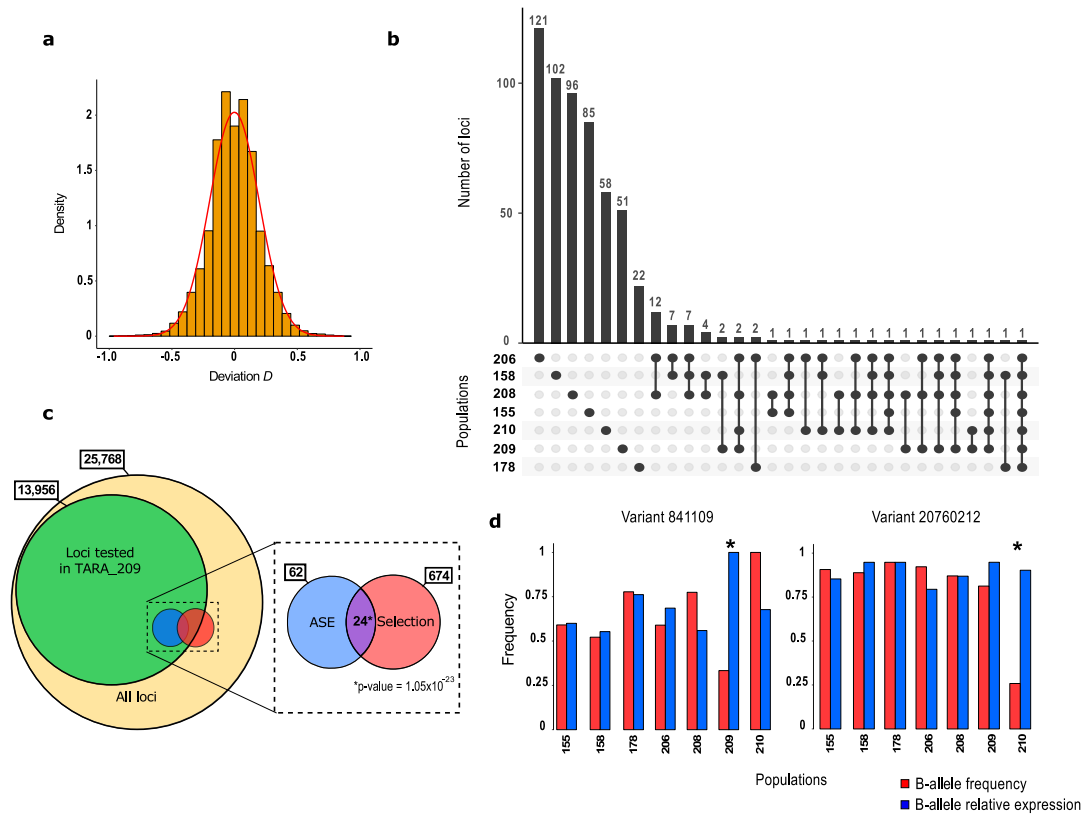


Figure 3: Population allele-specific expression detection and link with natural selection. **a**, The deviation  $D$  distribution in TARA\_209. The red line corresponds to the Gaussian distribution estimated from the data. **b**, Upset plot of the ASE detection in the seven populations. Each bar of the upper plot corresponds to the number of variants under ASE in the population(s) indicated by black dots in the lower plot. **c**, Crossing ASE and Selection. The yellow circle represents the total set of variants. In green, the number of heterozygous variants tested for ASE in TARA\_209. In blue and red, the amount of detected variants under ASE in TARA\_209 and under selection among the populations respectively. In purple, the intersection comprising variants under ASE in TARA\_209 and under selection, with its hypergeometric test p-value. **d**, Metagenomic and metatranscriptomic profiles of variants 841109 and 20760212. Each population is indicated on the x-axis, with the associated B-allele frequency (red) and B-allele relative expression (blue). The frequency is shown on the y-axis. The asterisks mean ASE was detected in the corresponding population.

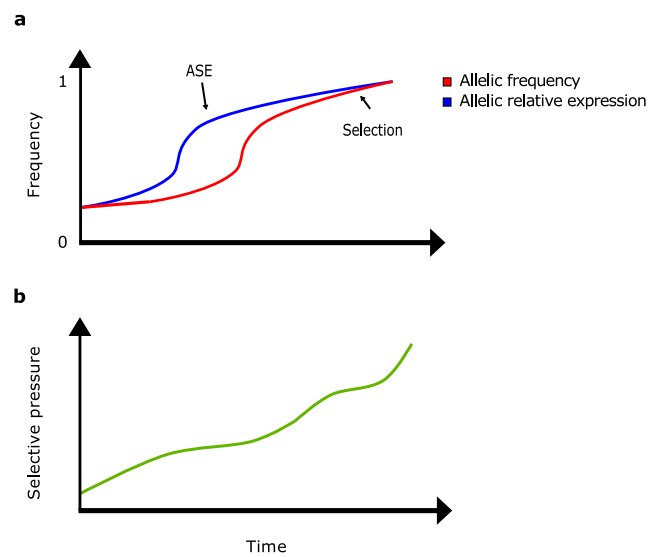


Figure 4: From allele-specific expression to natural selection. **a**, Evolution of allele frequency and allele relative expression over time. **b**, Evolution of selective pressure over time